# by Norton D. Lang

# Electronic structure and tunneling current for chemisorbed atoms

We discuss the tunneling current density in the vacuum region between two planar metal electrodes, one of which has an atom chemisorbed on its surface. The relation of this current distribution to the electronic structure of the adatom is analyzed. The study of this model problem leads to a better understanding of important aspects of the current flow in the scanning tunneling microscope. The emphasis of this work is not so much on the question of resolution discussed in other theoretical studies as on the characteristic signatures of chemically different atoms.

### Introduction

We consider here the distribution of tunneling current in the vacuum region between two planar metallic electrodes with a small bias voltage between them, in the instance in which there is an adsorbed atom at its equilibrium distance on one of the electrodes [1]. This analysis is designed to illuminate certain important aspects of the current flow in the scanning tunneling microscope [2–6].

For the metal surface we use the jellium model, which can be expected to be adequate for a general discussion of many

<sup>®</sup>Copyright 1986 by International Business Machines Corporation. Copying in printed form for private use is permitted without payment of royalty provided that (1) each reproduction is done without alteration and (2) the *Journal* reference and IBM copyright notice are included on the first page. The title and abstract, but no other portions, of this paper may be copied or distributed royalty free without further permission by computer-based and other information-service systems. Permission to *republish* any other portion of this paper must be obtained from the Editor.

of the properties that depend on the wave function well outside the surface. We begin with a brief outline of the calculation of the ground-state properties of an atom adsorbed on such a surface [7]. The density-functional theory of inhomogeneous electron systems, with the local-density approximation for exchange and correlation effects [8], is used in this calculation.

#### Adatom on metal surface

When an atom interacts with a system whose electronic states form a continuum, the discrete levels of the atom which are degenerate with the continuum broaden into resonances. The resonances formed in this way when Li, Si, and Cl atoms interact with a high-electron-density metal are shown in **Figure 1** (at their calculated equilibrium separations) [9]. The states constituting the Cl 3p resonance are below the Fermi level and are therefore occupied; those constituting the Li 2s resonance are mostly empty. This implies that charge transfer has taken place, toward the Cl atom and away from the Li atom, as would be expected from their electronegativities. The prohibitively large energy required either to fill or empty the Si 3p level forces this resonance to straddle the Fermi level, resulting in the formation of a covalent, rather than ionic, bond [10].

The electron densities [9] associated with the three fundamental bond types are exhibited for comparison in Figure 2. In the top row of the figure are presented contours of constant total electron density for the three adsorption systems. Note the way in which the contours rapidly regain their bare-metal form away from the immediate region of the atom. This is just a manifestation of the short range of metallic screening.

The detailed charge rearrangements associated with the atom-surface interaction are displayed in the bottom row of Figure 2, which gives contour maps of the difference between the electron density in the metal-atom system and the superposition of bare-metal and free-atom densities. The solid contours indicate regions of charge accumulation; broken contours indicate regions of charge depletion. These maps reflect the directions of charge transfer noted above.

#### Two-electrode system

Although we have available the self-consistent densityfunctional wave functions for a jellium surface with and without an adatom, we do not have them for the combined two-electrode system. Finding such wave functions for the combined system, from which we could directly determine the tunneling current, is a difficult problem. It would therefore seem useful to consider the Bardeen tunneling Hamiltonian formalism [11], which gives the total tunneling current in terms of wave functions determined separately for each electrode in the absence of the other. We wish, however, for purposes of our discussion to exhibit the current density distribution; therefore, the tunneling Hamiltonian formalism as it stands cannot be used. It proves possible though, via a derivation analogous to that of Bardeen, to obtain an expression for the current density in terms of the separate wave functions for the two electrodes.

We first describe the way in which we obtain our formula for the current density (using atomic units, in which h = m = |e| = 1). The Hamiltonian for the left (right) electrode considered separately is

$$H_{\rm L(R)} = -\frac{1}{2} \; \nabla^2 + \; V_{\rm L(R)};$$

 $H_{\rm L(R)}$  has eigenfunctions  $\psi_{\mu}^{\rm L}$  ( $\psi_{\nu}^{\rm R}$ ) and eigenvalues  $E_{\mu}$  ( $E_{\nu}$ ). The Hamiltonian for the combined (two-electrode) system is  $H=H_{\rm L}+V_{\rm R}$ . The wave function  $\Psi_{\mu}(\vec{r},t)$  for the combined system (whose form we need only in the vacuum region) is taken to coincide with  $\psi_{\mu}^{\rm L}$  at  $t=-\infty$  and to differ from it subsequently because of the adiabatic addition to  $H_{\rm L}$  of  $V_{\rm R}$ , regarded as a perturbation [12].

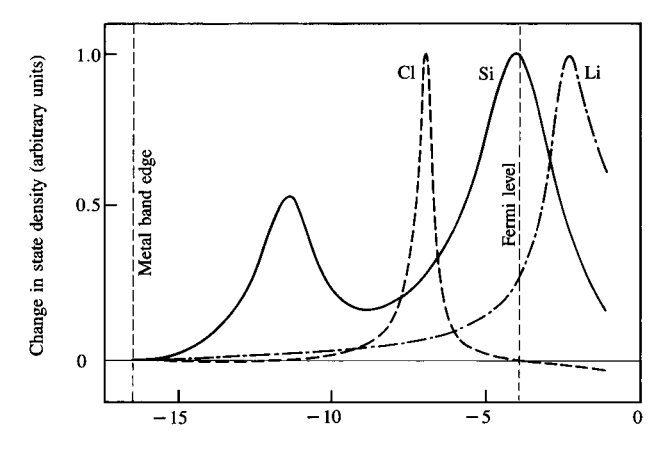
For small bias  $\mathscr{D}$  and zero temperature, the current density is

$$\vec{j}(\vec{r}) = 2 \mathcal{V} \int d\mu \ \delta(E_{\mu} - E_{\rm F}) \operatorname{Im} (\Psi_{\mu}^* \nabla \Psi_{\mu}). \tag{1}$$

(The factor 2 is for spins, which we do not include in our labels  $\mu$  and  $\nu$ .) We obtain  $\Psi_{\mu}(\vec{r},t)$  from the stationary eigenstates of  $H_L$  and  $H_R$  using time-dependent perturbation theory. In doing this we can of course just as well use  $\psi_{\mu}^{L*}$  in place of  $\psi_{\mu}^{L}$  (and similarly,  $\psi_{\nu}^{R*}$  in place of  $\psi_{\nu}^{R}$ ), and it proves convenient to extend the meaning of  $\int d\mu$  (and  $\int d\nu$  as well) to include a sum over these two cases. We then include a factor 1/2 with such integrals.

Now let us write

$$\tilde{J}_{\nu\mu}(\tilde{r}) = -\frac{1}{2} i(\psi_{\nu}^{R*} \nabla \psi_{\mu}^{L} - \psi_{\mu}^{L} \nabla \psi_{\nu}^{R*}). \tag{2}$$



Energy relative to vacuum (eV)

#### Figure 1

Curves of the difference in eigenstate density between the metaladatom system and the bare metal for adsorbed Li, Si, and Cl atoms. (The lower Si resonance corresponds to the 3s level; the corresponding level for Cl is a discrete state below the bottom of the metal band.) The metal electron density is 0.03 electrons/bohr<sup>3</sup> ( $r_s = 2$ ). (From [9]; reproduced with permission.)

Using the fact, demonstrated by Bardeen [11], that  $\langle \nu \mid V_R \mid \mu \rangle = i J_{\nu\mu}$ , where  $J_{\nu\mu} = \int d\vec{S} \cdot \vec{j}_{\nu\mu}(\vec{r})$ , with S a surface in the vacuum region, it can then be shown (see [1]) that

$$j(\vec{r}) = \pi \mathcal{V} \int d\mu \int d\nu \ \delta(E_{\mu} - E_{F}) \delta(E_{\nu} - E_{F}) J_{\nu\mu} j_{\nu\mu}^{*}(\vec{r}). \tag{3}$$

If this is integrated over the surface in the vacuum region, we recover the usual tunneling Hamiltonian expression for the total current [5]. (Note that there is a factor 1/4 here due to the redefinition of  $\int d\mu$  and  $\int d\nu$ .)

Now let us discuss briefly the computation of  $\psi^L$  and  $\psi^R$ . In the case of the bare metal in the jellium model (which we take as the right electrode),

$$\psi_{Em\kappa}^{R}(\vec{r}) = e^{im\phi} J_m(\kappa \rho) u_{E\kappa}(z), \tag{4}$$

where we use cylindrical coordinates with the z axis along the surface normal and where  $u_{E\kappa}(z)$ , which is computed self-consistently, is oscillatory deep in the metal and decays exponentially in the vacuum. The associated inverse decay length is given asymptotically by  $\sqrt{2\Phi + \kappa^2}$  in atomic units;  $\Phi$  is the electrode work function. This is discussed in [9]. Also described there are the self-consistently computed density-functional wave functions used to obtain Figure 2, but for that purpose they are only required within a sphere of ~7 bohr in radius about the atom. These wave functions (which we take as our  $\psi^L$ ) must for the present study be propagated further into the vacuum; this is done using the bare-metal Green's function described in [9]. Note that in evaluating Equation (3) to obtain the current density, the

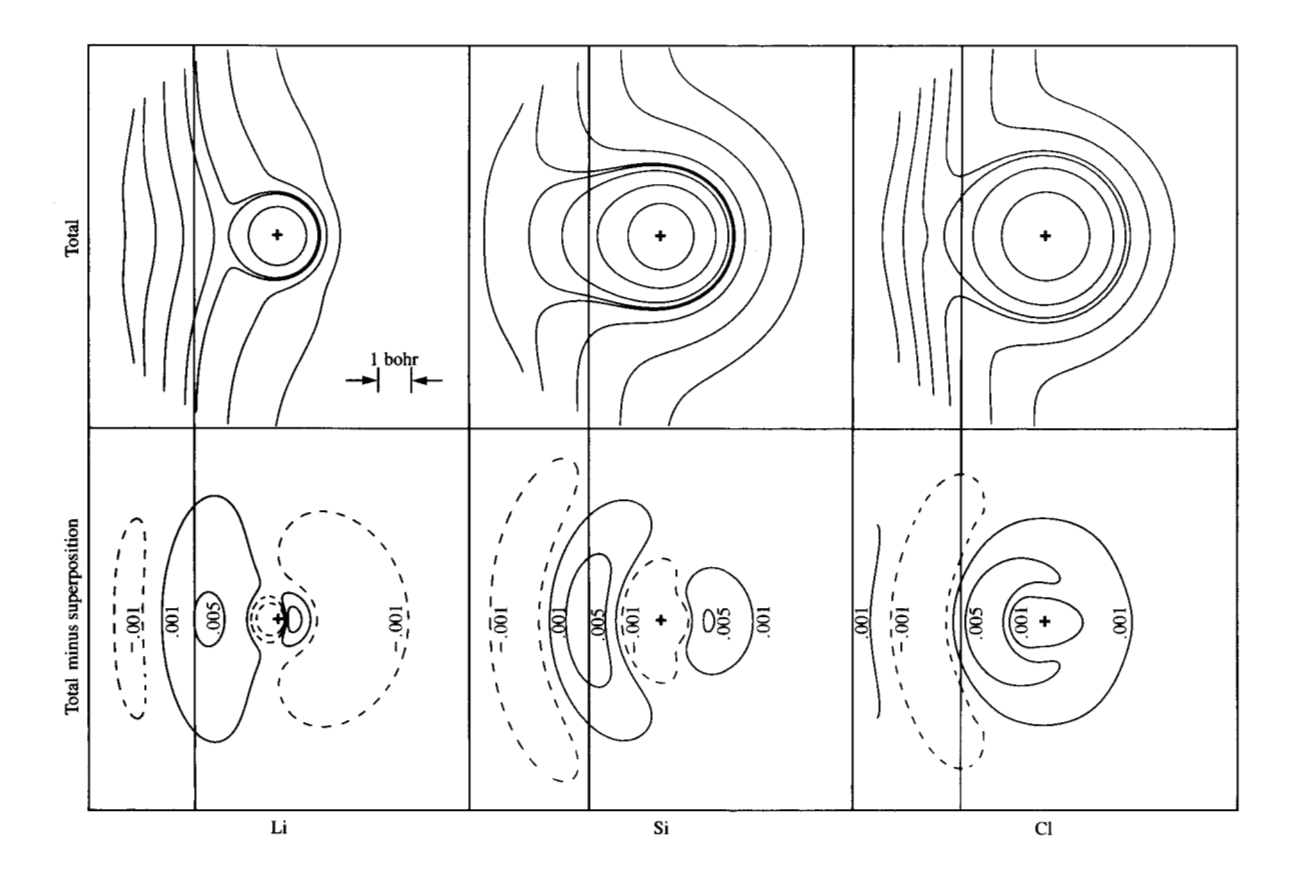


Figure 2

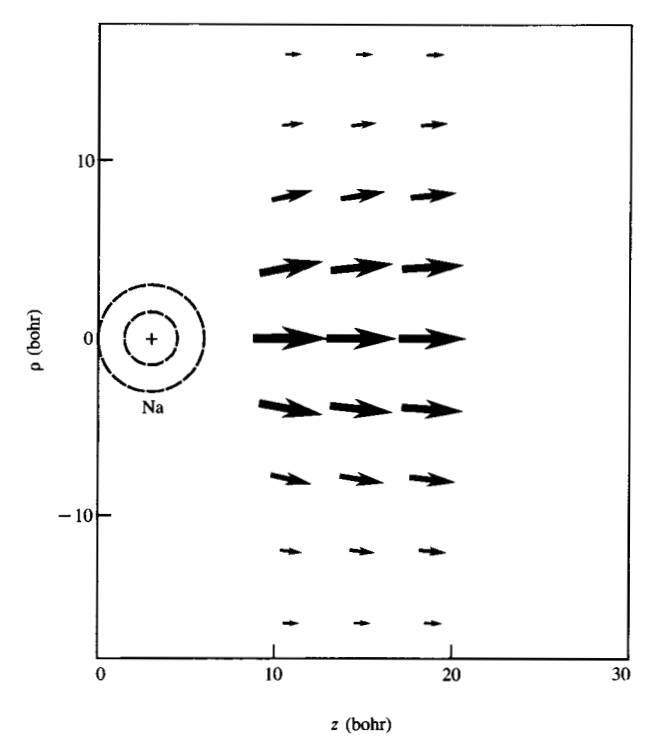
Top row: Contours of constant electron density in a plane normal to the metal surface containing the atom nucleus (indicated by +). The metal is at the left-hand side; the solid vertical line indicates the positive-background edge. Atoms are at their equilibrium distance from the metal. Contours are not shown outside the inscribed circle of each square; contour values are selected to be visually informative. Bottom row: Total electron density minus superposition of free-atom and bare-metal electron densities (electrons/bohr³). (From [9]; reproduced with permission.)

integrand (summand) will be diagonal in m (because of the cylindrical symmetry of our system) but not in  $\kappa$ , and so we must integrate over both  $\kappa_1$  and  $\kappa_R$  [13].

We now discuss our results. The two metallic electrodes are taken to have the same high electron density (corresponding to  $r_s = 2$ , which is broadly representative of many metals [14]). We first show the case in which a Na atom is adsorbed on the left electrode. The corresponding current density is shown in Figure 3. The left and right edges of the box correspond to the positive background edges for the two electrodes. The presence of the Na atom is indicated schematically by two dashed circles with a cross which gives the computed equilibrium distance of the nucleus. Results are shown only in a strip in the center of the vacuum barrier; much closer to the surfaces, the representation of the combined-system wave function  $\Psi$  in terms of  $\psi^L$  and  $\psi^R$  is not adequate. At each point of a grid in this strip, the current density is represented by an arrow. The length (and

thickness as well) of the arrow is made proportional to  $\ln (ej/j_0)$ , where j is the magnitude of the current density and  $j_0$  is the current density that would be present without the atom. The factor e = 2.718 is included so that at large lateral distances  $\rho$ , where  $j = j_0$ , we show a unit-length arrow instead of a blank space. Note for example that along the right edge of the strip the largest arrow represents roughly a factor of 25 in current density compared with the smallest arrow (which corresponds approximately to  $j_0$ ). The current distribution is quite sharp and shows a large enhancement due to the presence of the atom. The plate separation of 30 bohr (16 Å) is larger than the tip-to-surface separations presently typical of scanning tunneling microscope experiments. If we reduce the plate separation to, e.g., 16 bohr (8.5 Å), which is closer to a typical value, the current pattern (now computable reliably only in a narrower strip) is in fact quite similar to that seen in Figure 3. The additional tunneling conductance at this latter separation that is due to

376





Current density for the case in which a Na atom is adsorbed on the left electrode. The z and  $\rho$  directions are, respectively, normal and lateral to the surface. The lengths (and thicknesses) of the arrows are proportional to  $\ln (ej/j_0)$  evaluated at the spatial positions corresponding to the center of the arrows. (Corrects similar figure in [1].)

the presence of the atom is  $4 \times 10^{-8} \Omega^{-1}$  (which is near the experimental range). Figure 4 shows a contour map of  $j_z/j_0$  for the case given in Figure 3.

The dashed curve in the left half of Figure 5 shows the additional eigenstate density due to the presence of the Na atom on the metal surface which we have taken as our left electrode. The fact that the resonance, which corresponds to the 3s valence level of the free atom, is mostly above the Fermi level indicates that the 3s electron of the Na atom has been largely lost to the metal, as in the case of Li shown in Figures 1 and 2. In the present low-bias case only states in the immediate vicinity of the Fermi level contribute to the current; the density of such states is reduced because the peak of the resonance is significantly above the Fermi level. (Nonetheless there is still an appreciable density of 3s states at the Fermi level.)

We can study the cases for which the Fermi level lies higher in the s resonance by considering atoms in the next column of the periodic table. Instead of discussing Mg, which follows Na, we consider Ca, because it has the same calculated equilibrium metal-adatom separation as Na and thus our comparisons will not be complicated by the effects

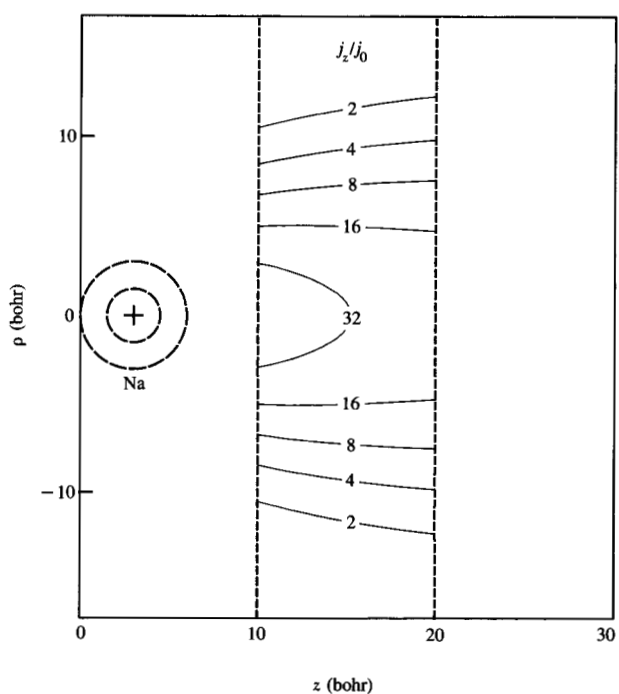
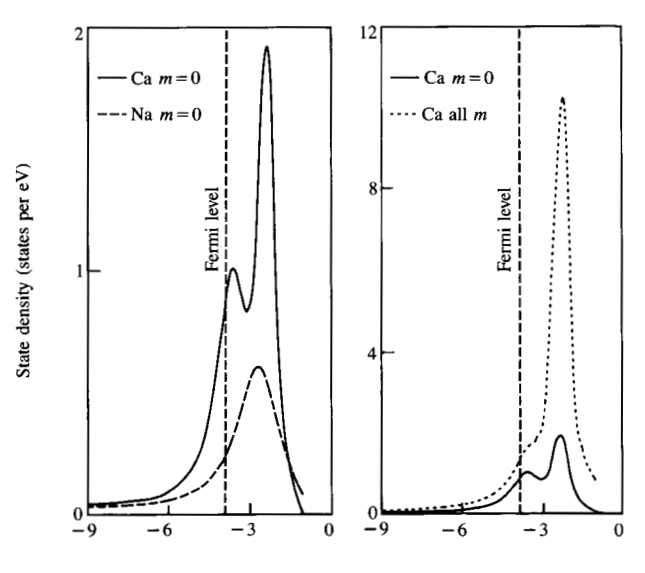


## Figure 4

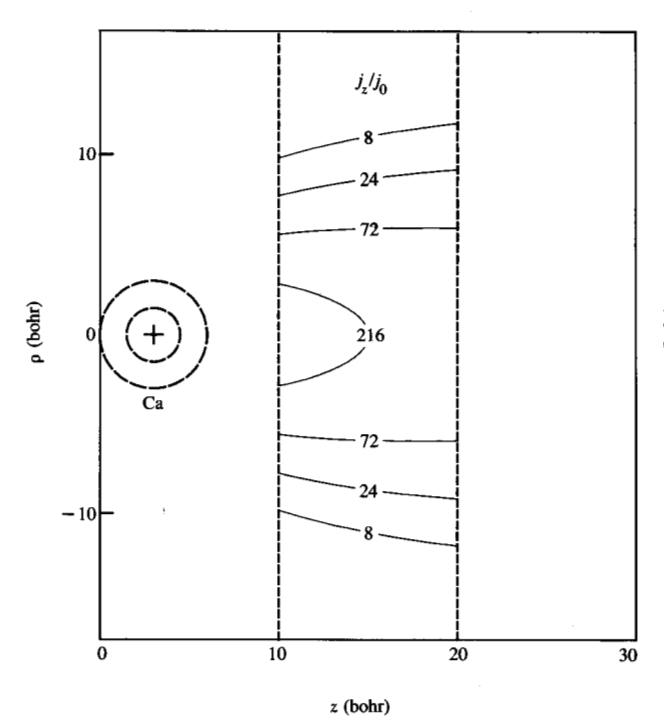
Contour map of  $j_z j_0$  for the case in which a Na atom is adsorbed on the left electrode. (Corrects similar figure in [1].)



Energy relative to vacuum (eV)

## Figure 5

Curves of the difference in eigenstate density between the metaladatom system and the bare metal for adsorbed Na and Ca atoms. The lower-energy Ca peak corresponds to the 4s state, the upper to 4p states (with some 3d-state contribution). The azimuthal quantum number is denoted by m. (From [1]; reproduced with permission.)



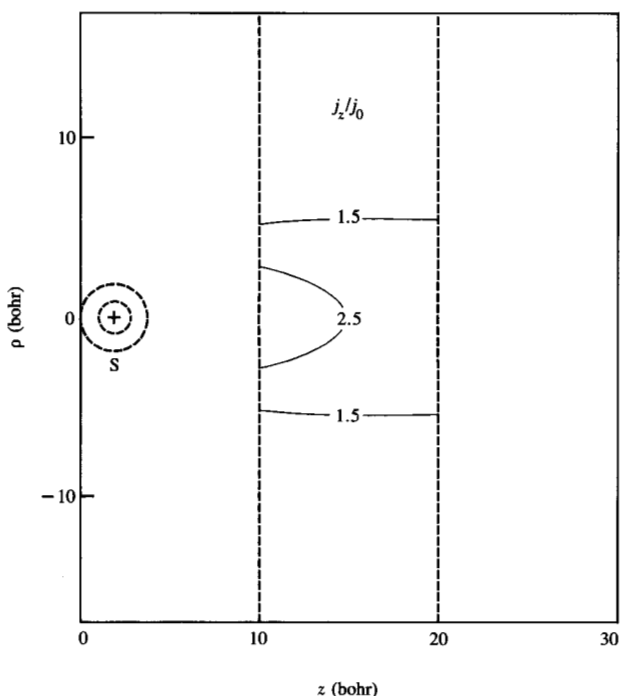


## Figure 6

Contour map of  $j_2/j_0$  for the case in which a Ca atom is adsorbed on the left electrode. (Corrects similar figure in [1].)

## Figure 7

Contour map of  $j_z/j_0$  for the case in which a S atom is adsorbed on the left electrode.

of changes in this separation. In the free atom, of course, the Ca 4s valence shell is filled, but in the adsorption case there is loss of electronic charge to the solid, with the result that the Fermi level is near the peak of the 4s resonance, as seen in the left half of Figure 5 (solid curve).

The calculations for the current distributions carried out here include wave functions of all m values [m] is the azimuthal quantum number; see Equation (4)]. Wave functions with  $m \neq 0$  (e.g.,  $p_{xy}$  states), however, have a node on the z axis, and as a consequence their main weight lies closer to the left electrode surface. Their contributions to the current are thus much smaller than those for m = 0 (e.g., s and  $p_z$  states), and in fact these  $m \neq 0$  wave functions make only a small contribution to the atom-induced current enhancement. For this reason, just the m = 0 contributions to the state densities are shown in the left part of Figure 5.

It is seen that the m=0 Fermi-level state density for Ca is approximately four times that for Na; and our computation shows that the total additional current due to the presence of the atom is larger by a similar factor ( $\sim$ 6). A contour map of  $j_z/j_0$  for Ca is shown in **Figure 6**. The right half of Figure 5 compares the state density computed for the Ca case including contributions from all m values with that for m=0 only. It is clear that the total state density (all m

included), as might be measured in a photoemission experiment, is potentially misleading in a discussion of tunneling currents.

Let us now continue our calculation for those atoms in the Na row of the periodic table where the p resonance of the adatom is largely below the Fermi level, and for which therefore the additional Fermi-level state density is very small. We find that the atom in such a case yields a current enhancement far smaller than would be expected from the distance the atom projects out from the surface. This is exemplified by the current-density map for S shown in Figure 7. This result emphasizes the fact that since a low-bias tunneling experiment only probes states near the Fermi level, most of the valence-p states, which give the atom its size, will not be visible in the experiment.

#### **Acknowledgments**

I am delighted to thank A. R. Williams, H. Rohrer, R. Landauer, M. Büttiker, T. D. Schultz, J. Tersoff, and D.-H. Lee for a number of helpful discussions.

## References and notes

- 1. N. D. Lang, *Phys. Rev. Lett.* **55**, 230 and 2925(E) (1985); **56**, 1164 (1986).
- G. Binnig, H. Rohrer, Ch. Gerber, and E. Weibel, *Phys. Rev. Lett.* 49, 57 (1982); 50, 120 (1983); A. M. Baro, G. Binnig,

- H. Rohrer, Ch. Gerber, E. Stoll, A. Baratoff, and F. Salvan, *Phys. Rev. Lett.* **52**, 1304 (1984).
- J. Tersoff and D. R. Hamann, Phys. Rev. Lett. 50, 1998 (1983); Phys. Rev. B 31, 805 (1985).
- N. Garcia, C. Ocal, and F. Flores, Phys. Rev. Lett. 50, 2002 (1983).
- 5. T. E. Feuchtwang, P. H. Cutler, and N. M. Miskovsky, *Phys. Lett.* **99A**, 167 (1983).
- E. Stoll, A. Baratoff, A. Selloni, and P. Carnevali, J. Phys. C 17, 3073 (1984).
- 7. For a general survey, see N. D. Lang, *Theory of the Inhomogeneous Electron Gas*, S. Lundqvist and N. H. March, Eds., Plenum Publishing Co., New York, 1983, pp. 309-389.
- P. Hohenberg and W. Kohn, *Phys. Rev.* 136, B864 (1964);
  W. Kohn and L. J. Sham, *Phys. Rev.* 140, A1133 (1965).
- 9. N. D. Lang and A. R. Williams, Phys. Rev. B 18, 616 (1978).
- 10. Cf. P. J. Feibelman, Phys. Rev. Lett. 54, 2627 (1985).
- 11. J. Bardeen, Phys. Rev. Lett. 6, 57 (1961).
- Cf. the discussion of C. B. Duke, *Tunnelling in Solids*, Solid State Physics Suppl. 10, H. Ehrenreich, F. Seitz, and D. Turnbull, Eds., Academic Press, Inc., New York, 1969, p. 209 ff.
- 13. Note also that we omit image effects in our calculation, and that we use the density-functional eigenfunctions as if they were *bona fide* single-particle wave functions.
- 14. The calculated work function is 3.9 eV, which is appropriate for an s-p metal of this density.

Received July 1, 1985; accepted for publication September 19, 1985

Norton D. Lang IBM Research Division, P.O. Box 218, Yorktown Heights, New York 10598. Dr. Lang received his Ph.D. from Harvard University in 1968. He joined IBM Research in 1969, after postdoctoral work at the University of California. He is a recipient of the 1977 Davisson-Germer Prize of the American Physical Society, and is a Fellow of the American Physical Society and the New York Academy of Sciences.